The early expansion of anergic NKG2A^{pos}/CD56^{dim}/CD16^{neg} natural killer represents a therapeutic target in haploidentical hematopoietic stem cell transplantation

Alessandra Roberto,[1*] Clara Di Vito,[2*] Elisa Zaghi,[2] Emilia Maria Cristina Mazza,[1,3] Arianna Capucetti,[2] Michela Calvi,[2] Paolo Tentorio,[2] Veronica Zanon,[1] Barbara Sarina,[4] Jacopo Mariotti,[4] Stefania Bramanti,[4] Elena Tenedini,[3] Enrico Tagliafico,[3] Silvio Bicciato,[3] Armando Santoro,[4] Mario Roederer,[5] Emanuela Marcenaro,[6] Luca Castagna,[4] Enrico Lugli[1,7*] and Domenico Mavilio[2,8*]

[1]Laboratory of Translational Immunology, Humanitas Clinical and Research Center, Rozzano, Milan, Italy; [2]Unit of Clinical and Experimental Immunology, Humanitas Clinical and Research Center, Rozzano, Milan, Italy; [3]Department of Life Sciences, University of Modena and Reggio Emilia, Modena, Italy; [4]Bone Marrow Transplant Unit, Humanitas Clinical and Research Center, Rozzano, Milan, Italy; [5]ImmunoTechnology Section, Vaccine Research Center, NIAID, NIH, Bethesda, MD, USA; [6]Dipartimento di Medicina Sperimentale (DI.ME.S.) and Centro di Eccellenza per le Ricerche Biomediche (CEBR) Università degli Studi di Genova, Italy; [7]Humanitas Flow Cytometry Core, Humanitas Clinical and Research Center, Rozzano, Milan, Italy and [8]Department of Medical Biotechnologies and Translational Medicine (BioMeTra), University of Milan, Italy

AR and CDV, EL and DM contributed equally to this work.

ABSTRACT

Natural killer cells are the first lymphocyte population to reconstitute early after non-myeloablative and T cell-replete haploidentical hematopoietic stem cell transplantation with post-transplant infusion of cyclophosphamide. The study herein characterizes the transient and predominant expansion starting from the second week following haploidentical hematopoietic stem cell transplantation of a donor-derived unconventional subset of NKp46[neg-low]/CD56^{dim}/CD16^{neg} natural killer cells expressing remarkably high levels of CD94/NKG2A. Both transcription and phenotypic profiles indicated that unconventional NKp46[neg-low]/CD56^{dim}/CD16^{neg} cells are a distinct natural killer cell subpopulation with features of late stage differentiation, yet retaining proliferative capability and functional plasticity to generate conventional NKp46^{pos}/CD56^{bright}/CD16[neg-low] cells in response to interleukin-15 plus interleukin-18. While present at low frequency in healthy donors, unconventional NKp46[neg-low]/CD56^{dim}/CD16^{neg} cells are greatly expanded in the seven weeks following haploidentical hematopoietic stem cell transplantation, and express high levels of the activating receptors NKG2D and NKp30 as well as of the lytic granules Granzyme-B and Perforin. Nonetheless, NKp46[neg-low]/CD56^{dim}/CD16^{neg} cells displayed a markedly defective cytotoxicity that could be reversed by blocking the inhibitory receptor CD94/NKG2A. These data open new and important perspectives to better understand the ontogenesis/homeostasis of human natural killer cells and to develop a novel immune-therapeutic approach that targets the inhibitory NKG2A check-point, thus unleashing natural killer cell alloreactivity early after haploidentical hematopoietic stem cell transplantation.

Introduction

The development over recent years of new protocols of allogeneic bone marrow transplant (BMT) arises from the need to rapidly identify a reliable source of hematopoietic stem cells (HSCs) to cure life-threatening hematologic malignancies. Indeed, the possibility of having a donor for nearly every patient requiring a

BMT pushed the optimization of different haploidentical HSC transplants (hHSCT) that combined different conditioned regimes and immune-modulation therapies.[1] Both myeloablative (MAC) and non-MAC (NMAC) T cell-replete (TCRe) hHSCT followed by post-transplant cyclophosphamide (Cy) gave remarkable positive clinical outcomes.[2-4]

Donor-derived immune-reconstitution (IR) is the most important player ruling out either a positive or negative clinical outcome of allogeneic HSCT.[5] Natural Killer (NK) cells are key for the prognosis of allogeneic BMT given their ability to kill viral-infected or tumor-transformed cells in the absence of a prior sensitization to specific antigens.[6-8] NK cell recognition of "self" relies on a large family of inhibitory NK cell receptors (iNKRs) including killer cell immunoglobulin-like receptors (KIRs) and C-type lectins, such as CD94/NKG2A, which specifically bind different alleles of major histocompatibility complex of class I (MHC-I). A decreased expression or lack of self-MHC-I on target cells unleash NK cell killing *via* the engagement of several activating NK cell receptors (aNKRs) (i.e., missing self hypothesis).[9-11] In the context of allogeneic and non-myeloablative BMT, the presence of a "mismatch" between iNKRs and HLA alleles on recipient cells induces a condition of alloreactivity that makes it possible for donor-derived NK cells to: i) eliminate recipient immune cells that survived the conditioning regimens (i.e., prevent graft reject), ii) kill recipient antigen presenting cells (APCs) presenting host antigens to donor T cells (i.e., avoid the onset of graft-*versus*-host disease [GvHD]), and iii) clear residual malignant cells in the recipient (i.e., induce graft-*versus*-leukemia [GvL] effect). These NK cell-mediated effector-functions in mismatched settings are being currently used to develop adoptive NK cell transfer therapies to cure solid and hematologic tumors.[7,12]

Circulating NK cell subsets are normally defined on the basis of CD56 and CD16 surface expression. Conventional CD56^{bright}/CD16$^{neg-low}$ (cCD56^{bright}) NK cells account for up to 10-15% of the total NK cell population, and are able to secrete a high amount of pro-inflammatory cytokines while displaying poor cytotoxicity. The conventional CD56^{dim}/CD16^{pos} (cCD56^{dim}) phenotype identifies another highly cytotoxic subset that comprises up to 90% of NK cells in the bloodstream.[13] Other than the pathologic NK subsets expanded in immunological disorders and in response to pathogens,[14] an additional population of unconventional CD56^{dim}/CD16^{neg} (uCD56^{dim}) NK cells has been identified recently.[15-17] Despite being rarely represented in healthy donors, uCD56^{dim} is highly cytotoxic and able to efficiently kill hematologic tumors *in vitro*.[18] A subset of CD56^{low}/CD16^{low} NK cells resembling the phenotype and functions of uCD56^{dim} NK cells is expanded in the bone marrow (BM) of healthy pediatric donors and leukemic patients who have undergone α/β T cell-depleted hHSCT.[18,19]

The study herein demonstrates that the NK cell IR in TCRe -NMAC-PT/Cy hHSCT with reduced intensity conditioning (RIC) are characterized by the early expansion of donor-derived and anergic uCD56^{dim} NK cells showing a peculiar NKG2A^{pos}/NKp46$^{neg-low}$ phenotype. We also demonstrate herein that the blocking of the NKG2A inhibitory pathway on this subset represents an immunotherapeutic target to improve NK cell alloreactivity early after hHSCT.

Methods

Study Design

30 patients were treated according to our published hHSCT protocol approved by the institutional review boards (IRB) of Humanitas Research Hospital.[20] Patients and donors signed consent forms in accordance with the Declaration of Helsinki. Patients' clinical features, enrolment criteria and timing of specimen collections are shown in the *Online Supplementary Table S1*.[21,22] Peripheral blood mononuclear cells (PBMCs) from healthy volunteers or patients were isolated as previously described.[22,23]

Flow cytometry and cell sorting

Cells were thawed in medium (Roswell Park Memorial Institute [RPMI]-1640 supplemented with 10% fetal bovine serum (FBS), 1% penicillin-streptomycin and 1% L-glutamine) containing benzonase nuclease (Sigma-Aldrich). Cells were stained for 15 minutes at room temperature (RT) with live/dead fixable dead cell stain kit (Life Technologies) and 20 minutes at RT with fluorescent-conjugated monoclonal antibodies (mAbs). All mAbs are listed in *Online Supplementary Table S2*. For Ki-67, Perforin and Granzyme (GRZ)-B intracellular staining, cells were fixed and permeabilized using the Cytofix/Cytoperm kit (BD Biosciences) according to the manufacturer's protocol. The gating strategy to identify NK cells within total PBMCs is shown in *Online Supplementary Figure S1*. Samples were acquired on a LSR Fortessa and LSR II flow cytometers or fluorescence-activated cell sorting (FACS)-sorted with FACS Aria III (BD Biosciences). NK cell absolute counts were obtained by calculating the percentage within the lymphocyte gate. Additional Methods are included in the *Online Supplementary Material*

Results

Preferential expansion of uCD56^{dim} NK cells in the first weeks after hHSCT

We identified CD14^{neg}/CD3^{neg}/CD20^{neg} NK cell subsets in peripheral blood (PB) and donor BM by polychromatic flow cytometry on the basis of their CD56 and CD16 surface expression within the lymphocyte gate.[13] We did not include CD56^{neg} or NKG2D^{neg} lymphocytes in our gating strategy, as these cells were contaminants lacking the NK cell surface markers NKp46, NKG2A, Perforin and Granzyme-B (*Online Supplementary Figure S1*). Our results showed that the absolute numbers of circulating NK cells in hHSCT recipients reach levels similar to those of their healthy donors within four to five weeks after hHSCT with a chimerism that is completely donor-derived after 28 days (Figure 1A,B). These findings confirmed that donor-derived NK cells represent the first lymphoid compartment to immune-reconstitute in allogeneic HSCT prior to T and B cells.[6,7,21,22,24,25]

We then characterized the dynamic of circulating NK cell subset IR early after hHSCT. Four distinct NK cell populations were detectable in both healthy donors and patients and their frequencies were remarkably different within the several time points examined. First, we observed that the frequency of cCD56^{bright} NK cells was significantly higher in the recipients compared to healthy donors starting from the third week from the transplant, and returned to similar physiologic levels 11 weeks after hHSCT. Conversely, the percentage of the cCD56^{dim} NK cells was very low, if not undetectable, in the recipients within the same period, and returned similar to that of their related donors five months after the transplant. The

low levels of cCD56^{dim} NK cells early after hHSCT were counterbalanced by a significant expansion the uCD56^{dim} NK cell subset which, instead, was present at low levels in PB under homeostatic conditions. uCD56^{dim} NK cells started to statistically increase in the recipients compared to their related donors in the second week after the transplant, outnumbered all other NK cell subsets in the second and third week, and returned to normal level only eight weeks after hHSCT. Different from Human Leukocyte Antigen (HLA)-matched HSCT,[26] CD56^{bright}/CD16^{pos} NK cells did not increase in frequency at any time-point in

hHSCT recipients compared to their related donors (Figure 1C,D). We and others have reported that the infection/re-activation with human cytomegalovirus (HCMV) greatly influences the homeostasis and ontogenesis of NK cell subset and induces the expansion of CD56^{neg}/CD16^{pos} NK cells. This phenomenon is particularly relevant in the immune-compromised recipients receiving allogeneic HSCT.[14] Although 23 of the 30 (77%) transplanted patients recruited for this study experienced a HCMV infection/reactivation starting from day 29 post hHSCT up to day 64 following the transplant (*Online*
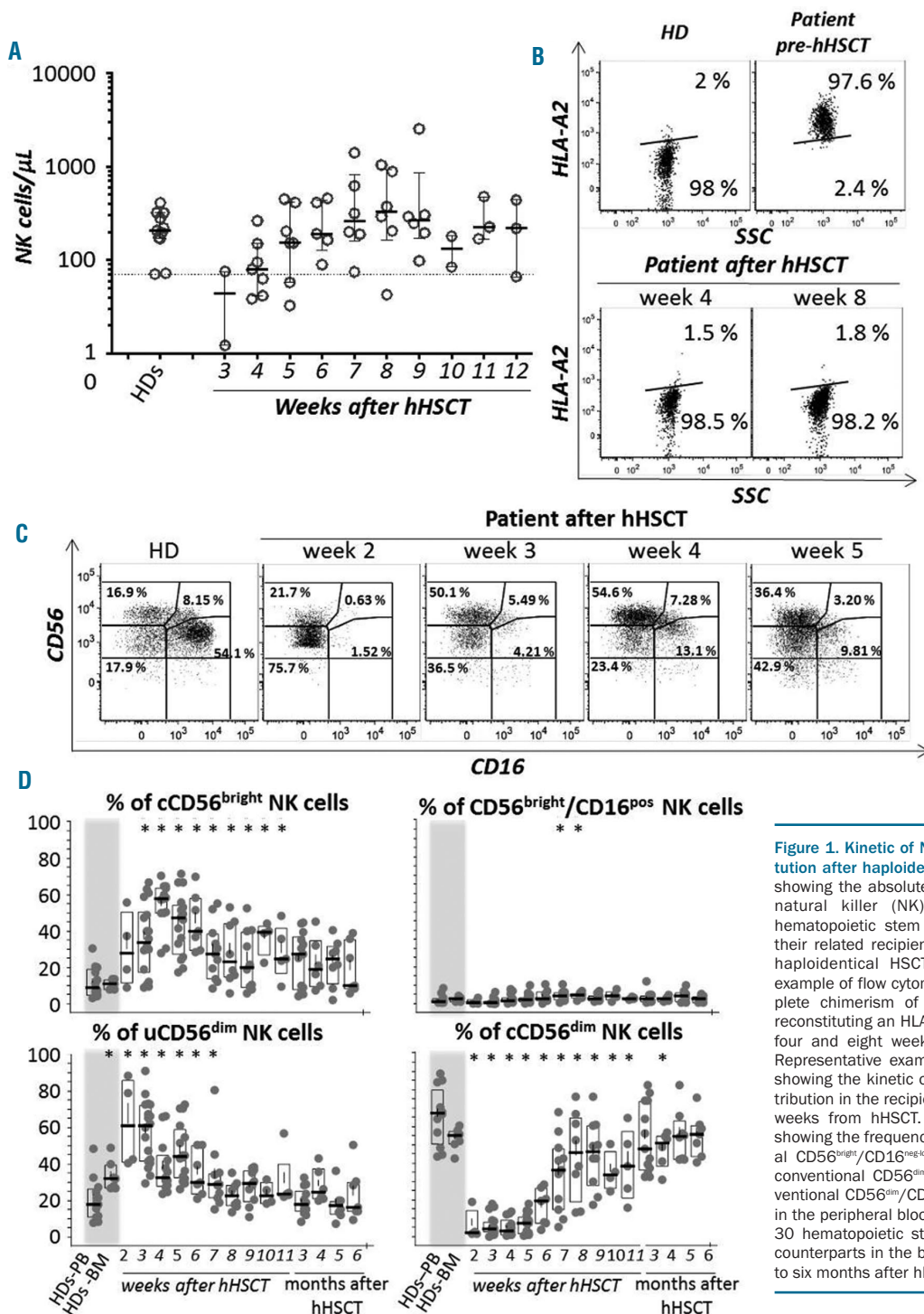

Figure 1. Kinetic of NK cell subset immune reconstitution after haploidentical HSCT. (A) Summary graph showing the absolute counts (cells/µL) of circulating natural killer (NK) cells (mean ± SEM) from hematopoietic stem cell healthy donors (HDs) and their related recipients at different time-points after haploidentical HSCT (hHSCT). (B) Representative example of flow cytometry dot plots showing the complete chimerism of HD-derived HLA-A2^{neg} NK cells reconstituting an HLA-A2[pos] recipient (upper line) after four and eight weeks from hHSCT (lower line). (C) Representative example of flow cytometry dot plots showing the kinetic of HD-derived NK cell subset distribution in the recipient after two, three, four and five weeks from hHSCT. (D) Summary statistical graph showing the frequency (median ± SEM) of conventional CD56^{bright}/CD16[neg-low] (cCD56^{bright}), CD56^{bright}/CD16^{pos}, conventional CD56^{dim}/CD16^{pos} (cCD56^{dim}) and unconventional CD56^{dim}/CD16^{neg} (uCD56^{dim}) NK cell subsets in the peripheral blood (PB) and bone marrow (BM) of 30 hematopoietic stem cell HDs compared to their counterparts in the blood of the related recipients up to six months after hHSCT. *P<0.05.

Supplementary Table S1), neither the frequency (*Online Supplementary Figure S2A*) nor the phenotype (*data not shown*) of uCD56^{dim} NK cells were affected over time by this viral infection.

Even though the existence and the functional relevance of uCD56^{dim} NK cells have been previously reported,[15-17] a recent study claimed that the CD56^{dim}/CD16^{neg} phenotype is induced by cryopreservation.[27] To further validate our experimental results performed on cryopreserved cells, we compared the distribution of NK cell subsets between freshly isolated and thawed PBMCs from healthy donors and transplanted patients. Our results showed that both frequencies and phenotypes of the four NK cell subsets from cryopreserved PBMCs are similar to those of freshly purified ones (*Online Supplementary Figure S2B-D*).

uCD56^{dim} lymphocytes are *bona fide* NK cells

To confirm that CD14^{neg}/CD3^{neg}/CD20^{neg} uCD56^{dim} lymphocytes are indeed NK cells, polychromatic flow cytometry data from 11 healthy donors and from five patients purified three weeks after hHSCT were labelled with a unique computational barcode, concatenated and analyzed by the t-distributed Stochastic Neighbor Embedding (t-SNE) algorithm.[28] We arbitrarily identified 13 different clusters (from C1 to C13) of non-T and non-B lymphocytes on the basis of population boundaries distinguishable on the t-SNE density plots (Figure 2A). We then determined the frequency of antigen expression in each cluster by manual gating (*Online Supplementary Figure S3*), and displayed the results using a heat map. Figure 2B shows that all clusters except C13 harbor several NK cell surface markers at different degrees of expression. cCD56^{bright}, cCD56^{dim} and uCD56^{dim} NK cell subsets overlap across the distinct clusters defined in the t-SNE map and show a similar distribution in healthy donors and hHSCT recipients (Figure 2C,D). cCD56^{bright} are composed of C7, C8, C9 and, as expected, are NKp46^{pos} and NKG2A^{pos} while expressing low levels of Granzyme-B and Perforin. cCD56^{dim} NK cells are present at higher frequencies in healthy donors compared to hHCST recipients and belong to C3, C4, C5, and C6 groups. These cells are characterized by constitutive high expressions of Granzyme-B and Perforin. uCD56^{dim} cells are comprised of C10, C11, C12 and are NKp46$^{neg-low}$, NKG2D^{pos}, Granzyme-B^{pos} and Perforin^{pos} (Figure 2E). This high-dimensional approach of polychromatic flow cytometry data analysis, although applied to a small number of hHSCT patients, indicate that uCD56^{dim} cells are *bona fide* NK cells.
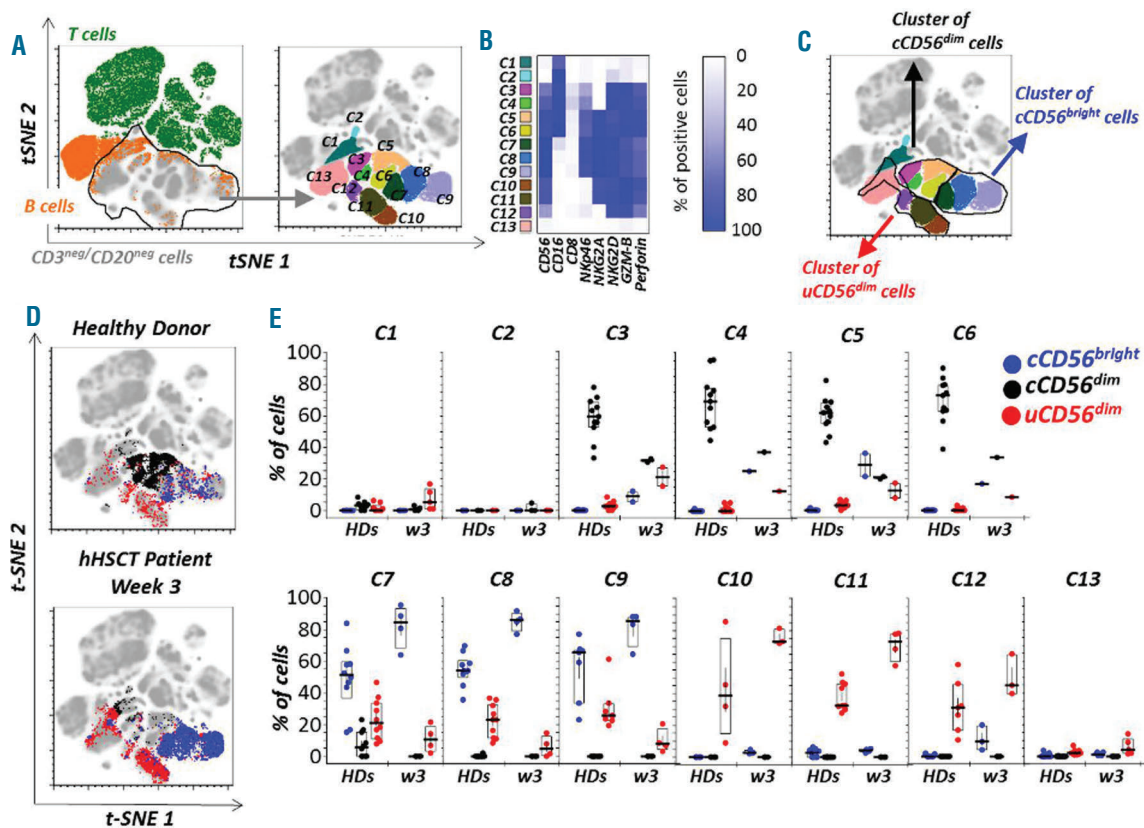

Figure 2. Clustering of uCD56^{dim} NK cells. (A) t-distributed Stochastic Neighbor Embedding (t-SNE) plot of lymphocytes from 11 healthy donors (HDs) and five recipients at three weeks after haploidentical HSCT (hHSCT). CD3^{pos} T (green on the left plot) and CD20^{pos} B (orange on the left plot) cells are grouped within the t-SNE map. Within the CD3^{neg}/CD20^{neg} gate (gray within the left plot), 13 (from C1 to C13) different clusters of lymphocytes were defined based on the population boundaries (right plot). (B) Heatmap showing the degree of expression of CD56, CD16, CD8, NKp46, NKG2A, NKG2D, Granzyme-B (GRM-B) and Perforin on the 13 clusters of non-T and non-B lymphocytes defined in the right t-SNE plot of panel A. (C-D) t-SNE plots showing, within the 13 CD3^{neg}/CD20^{neg} clusters of lymphocytes presented in panel B, the clusters of cCD56^{bright} (blue), cCD56^{dim} (black) and uCD56^{dim} (red) NK cell subsets from HDs and from hHSCT-patients three weeks after HSCT together (C) or separately (D). (E) Graphs showing the frequencies (median ± SEM) of cCD56^{bright}, cCD56^{dim} and uCD56^{dim} from HDs and patients at three weeks after hHSCT (w3) out of the total cells in each of the 13 clusters of CD3^{neg}/CD20^{neg} lymphocytes.

uCD56^{dim} NK cells are not NK cell precursors and express low levels of NKp46

Ontogenetically, human NK cell precursors have been divided into three main differentiation stages on the basis of their different expression of several surface markers, including CD34, CD117 and CD127. These precursors give rise first to cCD56^{bright} (stage 4) and then to terminally differ-entiated cCD56^{dim} (stage 5) NK cell subsets that are characterized by a CD34^{neg}/CD117^{neg}/CD127^{neg} phenotype and express aNKRs (i.e., NKG2D and natural cytotoxicity receptors [NCRs]).[29,30] Our data showed that uCD56^{dim} NK cells from both healthy donors and hHSCT patients are NKG2D^{pos} and NKp30^{pos}, but do not express CD34, CD117 and CD127, thus proving that they are NK cells in later
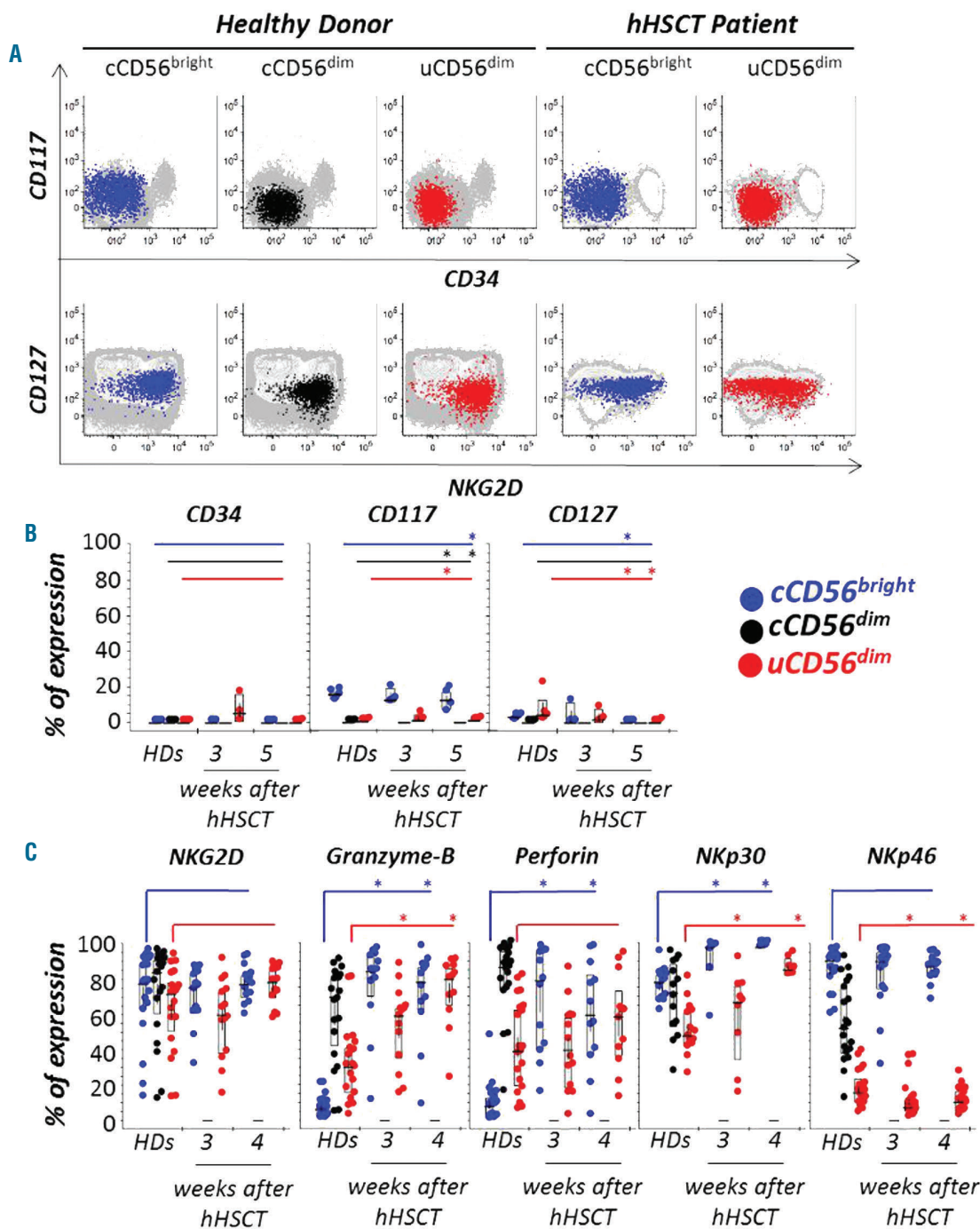

Figure 3. Phenotype of NK cell subsets in healthy donors and haploidentical HSCT patients. (A) Representative example of flow cytometry dot plots from a healthy donors (HDs) and a patient after three weeks from haploidentical HSCT (hHSCT) showing the surface expression of CD117, CD34, CD127 and NKG2D on cCD56^{bright} (blue), cCD56^{dim} (black) and uCD56^{dim} (red) NK cells. The phenotypes of these representative NK cell subsets are overlaid with those of their viable lymphocytes (gray background) used as positive controls. (B) Summary statistical graph showing the expression of CD34, CD117 and CD127 on cCD56^{bright} (blue), cCD56^{dim} (black) and uCD56^{dim} (red) from three HSC HDs and their recipients at three and five weeks after hHSCT. (C) Summary statistical graph showing the expression of NKG2D, Granzyme-B, Perforin, NKp30, NKp46 on cCD56^{bright} (blue), cCD56^{dim} (black) and uCD56^{dim} (red) from HSC HDs and their recipients after three and four weeks from hHSCT. *$P<0.05$

stages of differentiation rather than NK cell precursors (Figure 3A,B). In line with their previously reported high cytotoxicity,[18] we also observed that uCD56^{dim} NK cells express high levels of Perforin and Granzyme-B. Interestingly, we also found that uCD56^{dim} NK cells have low levels of NKp46, thus making this NCR an additional phenotypic marker capable of distinguishing the latter subset from both cCD56^{bright} and cCD56^{dim} NK cells (Figure 3C).

uCD56^{dim} NK cells expanded early after hHSCT have a unique transcriptional profile

To gain more insights into the biological and functional relevance of uCD56^{dim} NK cells, we assessed the gene expression profiles of FACS-sorted circulating NK cell subsets from three healthy donors (three replicates for each of the three cCD56^{bright}, cCD56^{dim} and uCD56^{dim} NK cell subsets) and from their three hHSCT recipients (three replicates for each of the two cCD56^{bright} and uCD56^{dim} NK cell subsets) three weeks after the transplant. In order to reduce data dimensionality in three main directions, we

first analyzed our results *via* the principal component analysis (PCA) algorithm. PCA showed that the transcriptional signatures of NK cell subsets from healthy controls are different from those of hHSCT patients (Figure 4A). Moreover, the gene set enrichment analysis (GSEA) performed on healthy donors and hHSCT patients indicates that the majority of the gene sets enriched in the recipients are associated with cell cycle, DNA repair and ribonucleic acid (RNA) transcription (false discovery rate [FDR] <0.00001) (*Online Supplementary Table S3*). Hence, donor-derived NK cells early after hHSCT are activated and endowed with high proliferative potential.

We then analyzed the gene expression of cCD56^{bright}, uCD56^{dim} and cCD56^{dim} NK cells from healthy donors, and determined that 3072 transcripts are differentially expressed between these three NK cell subsets. These different transcriptional profiles were then compared with those of uCD56^{dim} and cCD56^{bright} NK cells from patients. Indeed, these latter two NK cell subsets were the only ones to have expanded and be detectable three weeks
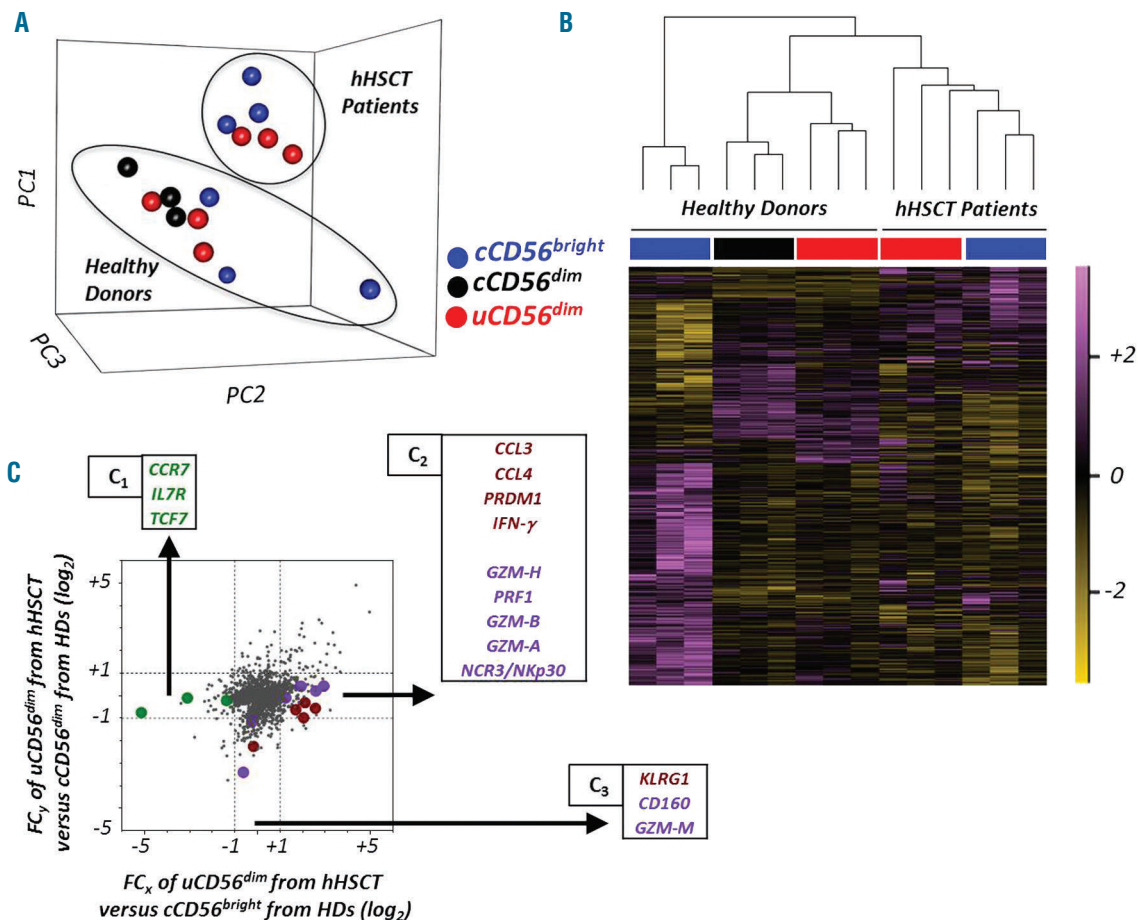

Figure 4. Transcriptional profiles of NK cell subsets from healthy donors and patients three weeks after haploidentical HSCT. (A) Principal component analysis (PCA) showing the gene expression profiles of cCD56^{bright}, cCD56^{dim} and uCD56^{dim} NK subsets from healthy donors (HDs) and of cCD56^{bright} and uCD56^{dim} from patients after three weeks from haploidentical HSCT (hHSCT). (B) Hierarchical clustering of NK cell subsets from healthy donors and patients three weeks after hHSCT. Sample grouping, obtained from the expression levels of 3072 genes that are differentially expressed between cCD56^{bright}, uCD56^{dim} and cCD56^{dim} NK cells from HDs. Yellow and violet colors indicate decreased and increased expression, respectively. (C) Log$_2$ expression fold-change (FC) in uCD56^{dim} from hHSCT patients *versus* cCD56^{bright} cells (x-axis), and *versus* cCD56^{dim} cells (y-axis) from HDs. C1 and C2 boxes indicate the genes similarly expressed with cCD56^{dim} from HDs but downregulated (C1) and upregulated (C2) in uCD56^{dim} from hHSCT *versus* cCD56^{bright} from HDs. C3 box indicates the genes downregulated in uCD56^{dim} from hHSCT *versus* cCD56^{dim} from HDs and similarly expressed with cCD56^{bright} from HDs. Downmodulated genes highlighted in green and upmodulated genes highlighted in red are associated with NK cell maturation, genes highlighted in violet are associated with NK cell activation or cytotoxicity.

after the transplant (Figure 1C,D). Supervised hierarchical clustering revealed that in healthy donors uCD56^{dim} NK cells have a gene expression similar to that of cCD56^{dim} cells and different from that of cCD56^{bright} NK cells. These results were somewhat expected considering that both uCD56^{dim} and cCD56^{dim} NK cells share a high degree of cytotoxicity in physiological conditions.[2] Although showing distinct gene expression profiles, cCD56^{bright} and uCD56^{dim} NK cells from hHSCT recipients group together and are more similar to cCD56^{dim} than cCD56^{bright} NK cell subsets from healthy donors (Figure 4B).

We then compared the fold change (FC) of the 3072 differentially expressed genes between uCD56^{dim} NK cells from hHSCT patients and cCD56^{bright} (FCx) or cCD56^{dim} (FCy) NK cells from healthy donors (Figure 4C). Among those transcripts of uCD56^{dim} NK cells from hHSCT patients similarly expressed in cCD56^{dim} NK cells from healthy donors (FCy ($\log_2$) < |1|) but differently modulated in cCD56^{bright} NK cells from healthy donors (FCx ($\log_2$) > |1|), we found a downregulation of *CCR7*, interleukin *(IL)-7R* and *TCF7* (Figure 4C$_1$) as well as an upmodulation of *CCL3*, *CCL4*, *PRDM1* and *IFN-γ* (Figure 4C$_2$). Furthermore, uCD56^{dim} NK cells from hHSCT patients show an increased gene expression of *NKp30*, *Perforin (PRF)*, *Granzyme (GRZ-B)*, *GRZ-A* and *GRZ-H* compared to cCD56^{bright} NK cells from healthy donors (Figure 4C2). Among those transcripts of uCD56^{dim} NK cells from hHSCT patients similarly expressed in cCD56^{bright} NK cells

from healthy donors (FCx ($\log_2$) < |1|) but differently modulated in comparison with cCD56^{dim} NK cells from healthy donors (FCy ($\log_2$) > |1|) we found a downregulation of the maturation marker *KLRG1* (Figure 4C$_3$), of *CD160* and *GRZ-M* (Figure 4C$_3$).

These transcriptional profiles parallel our flow cytometry data and confirmed our working hypothesis postulating that uCD56^{dim} NK cells present at high frequencies early after hHSCT are not NK cell precursors, but rather represent lymphocytes in a later stage of differentiation whose gene expression profile is intermediate between cCD56^{bright} and cCD56^{dim} NK cells.

Highly proliferating NKp46[neg-low]/uCD56^{dim} cells can generate NKp46^{pos}/cCD56^{bright} NK cells

Donor-derived uCD56^{dim} and cCD56^{bright} NK cell subsets expressed high levels of Ki-67 (i.e., proliferating) at three and four weeks after hHSCT, while their counterparts in healthy donors were all Ki-67^{neg} (i.e., quiescent) (Figure 5A). These high rates of NK cell proliferation in hHSCT are associated with the so-called "cytokine storm" which occurs early after allogeneic transplant and induces immune cell activation and differentiation to rapidly recuperate the recipients from the previously induced and life-threatening condition of immunodeficiency.[25,31] The preferential expansion of Ki67^{pos}/uCD56^{dim} NK cells starting from the second week after hHSCT prompted us to hypothesize that they could generate either cCD56^{bright} or cCD56^{dim}
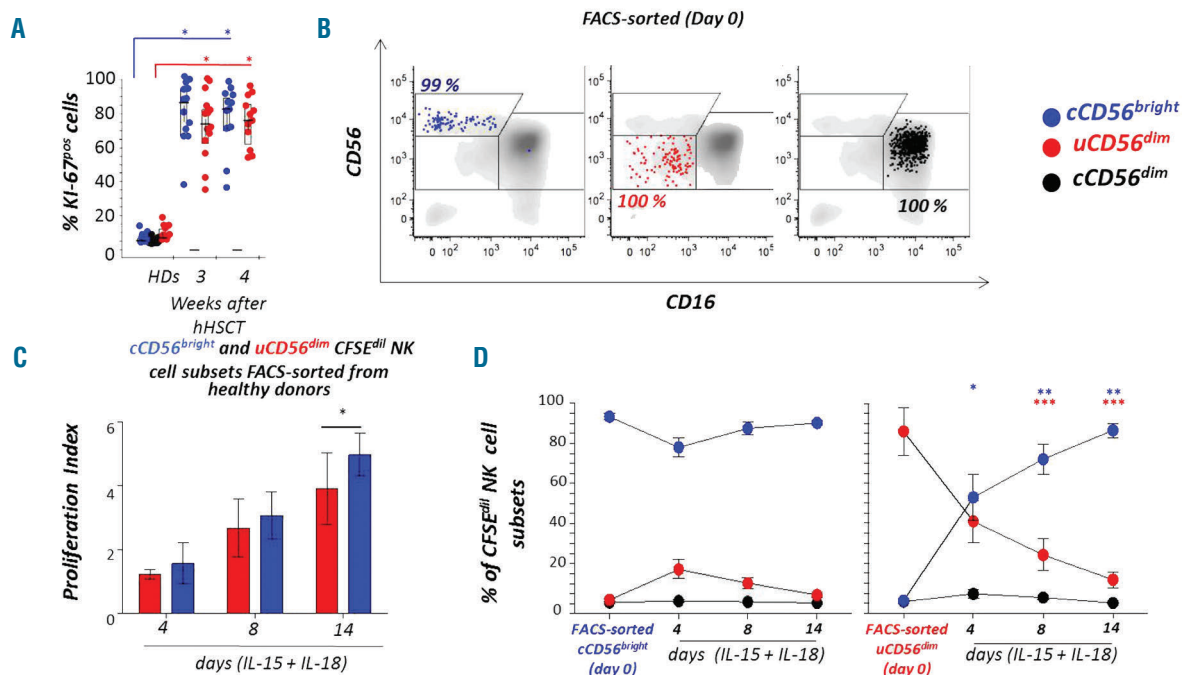

Figure 5. FACS-sorted uCD56^{dim} NK cells generate cCD56[br] NK cells under IL-15 and IL-18 stimulation. (A) Summary statistical graph showing the expression of Ki67 on cCD56^{bright} (blue), cCD56dim (black) and uCD56^{dim} (red) from HSC healthy donors (HDs) and their recipients after three and four weeks from hHSCT. (B) Representative example from a HD of flow cytometry dot plots showing the purity of fluorescence-activated cell sorting (FACS)-sorted cCD56^{bright} (blue), cCD56^{dim} (black) and uCD56^{dim} (red) (left column) natural killer (NK) cell subsets. Highly pure and FACS-sorted NK cell subsets are overlaid with the phenotype of purified CD3^{neg}/CD20^{neg} NK cells expressing CD56 and CD16 (gray). (C) Summary statistical graphs showing the proliferation index of FACS-sorted cCD56^{bright} (blue) and uCD56^{dim} (red) NK cell subsets from six HDs at four, eight and 14 days of culture with interleukin (IL)-15+ IL-18. (D) Summary statistical graph showing the kinetic of CFSE-diluting (CFSE[dil]) cCD56^{bright} (blue), cCD56^{dim} (black) and uCD56^{dim} (red) NK cell subsets generated from FACS-sorted cCD56^{bright} (upper panel) and uCD56^{dim} (lower panel) from seven HDs. No data are available for the cCD56^{dim} NK cells, as they were not proliferating in response to IL-15 and IL-18. Data are expressed as means ± S.D. *P<0.05; **P<0.01; ***P<0.001.

NK cells, whose frequencies in the recipient PB increase over the following weeks (Figure 1C,D). To validate this working hypothesis, we FACS-sorted uCD56^{dim}, cCD56^{bright} and cCD56^{dim} NK cells from healthy donors (Figure 5B), cultured them with IL-15 plus IL-18 and analyzed the phenotype of proliferating cells diluting carboxyfluorescein succinimidyl ester (CFSE) at several time points. IL-15 was chosen on the basis of its enhanced ability to prime NK cell proliferation and because it is increased significantly in the blood of the recipient receiving allogeneic (including haploidentical) HSCT.[25,31,32] Similarly, IL-18 is known to have a deep impact on NK cell activation and effector-functions.[33,34] In this regard, our transcriptional data showed that IL-18 receptor-1 (*IL-18-R1*) is significantly upregulated in uCD56^{dim} NK cells from hHSCT patients compared to cCD56^{dim} NK cells from healthy donors (FCy (log$_2$) > |1|) (*Online Supplementary Table S4*). In line with our transcriptional data (Figure 4), we first observed that both uCD56^{dim} and cCD56^{bright} NK cells highly proliferate in response to IL-15 and IL-18, while terminally differentiated cCD56^{dim} NK cells do not. The proliferation index of cCD56^{bright} NK cells is significantly higher after 14 days of culture compared to those of uCD56^{dim} NK cells (Figure 5C and *data not shown* for

cCD56^{dim} NK cells). Given the differential expression of NKp46 on uCD56^{dim} and cCD56^{bright} NK cells (Figure 3C), we analyzed the surface levels of this NCR to track the fate of these two proliferating subsets. Although cycling at a higher rate, only a minor and not statistically significant fraction of FACS-sorted NKp46^{pos}/cCD56^{bright} NK cells generated NKp46$^{neg-low}$/uCD56^{dim} NK cells over time. Indeed, the phenotype of proliferating cCD56^{bright} NK cells was similar (range 75-95%) to that of their resting and parental counterparts at day 0. On the other hand, almost all proliferating NKp46$^{neg-low}$/uCD56^{dim} NK cells gave rise to NKp46^{pos}/cCD56^{bright} NK cells after 14 days of culture, and only a minor fraction retained the NKp46$^{neg-low}$/uCD56^{dim} phenotype. Finally, we observed that neither FACS-sorted NKp46^{pos}/cCD56^{bright} NK cells nor FACS-sorted NKp46$^{neg-low}$/uCD56^{dim} NK cells were able to generate cCD56^{dim} NK cells (Figure 5D and Figure 6).

uCD56^{dim} cells expanded early after hHSCT are anergic due to high expression of NKG2A

Our phenotypic analyses showed that donor-derived uCD56^{dim} NK cells expanded early after hHSCT patients are fully armed to efficiently kill tumor cell targets, as already demonstrated in healthy donors.[18] Surprisingly,
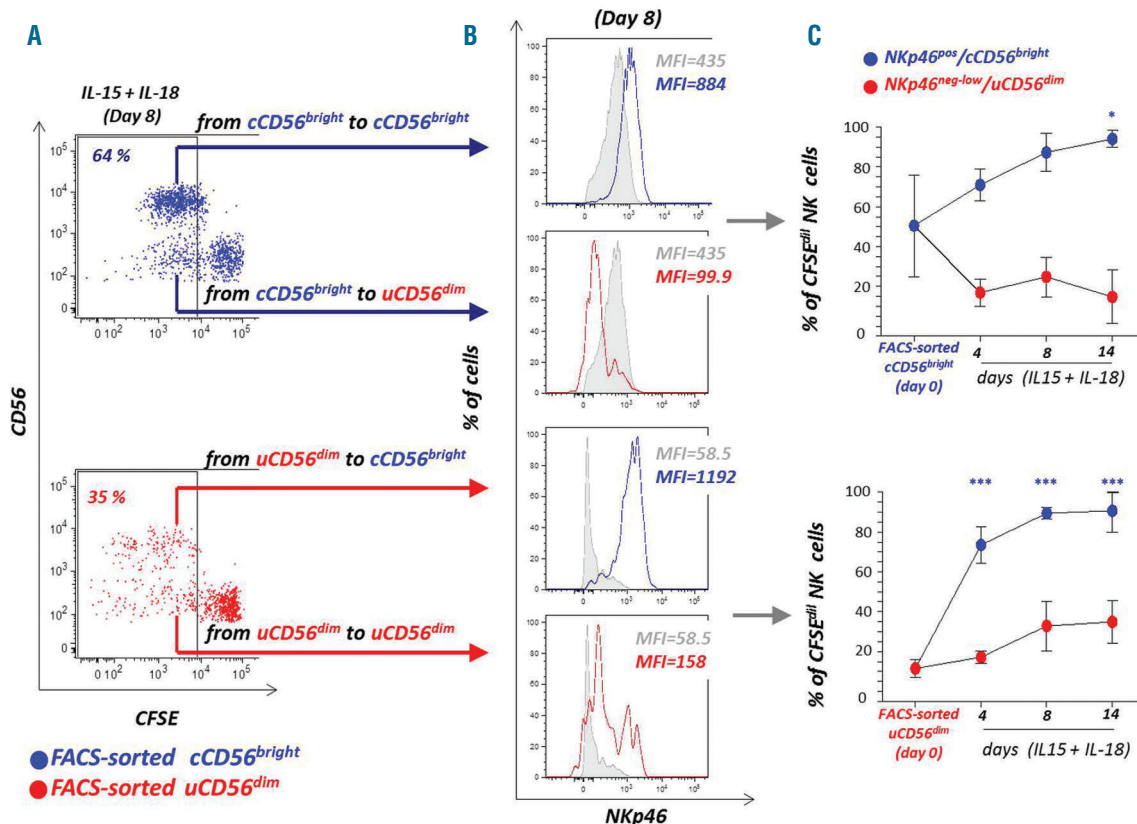

Figure 6. Proliferating NKp46$^{neg-low}$/uCD56^{dim} NK cells differentiate in NKp46^{pos}/cCD56^{bright} NK cells. A) Representative example from a HD of flow cytometry dot plots showing the expression of CD56 on fluorescence-activated cell sorting (FACS)-sorted and CFSE-diluting (CFSE^{dil}) cCD56^{bright} (blue) and uCD56^{dim} (red) from a HD after eight days in culture with interleukin (IL)-15 + IL-18. (B) Representative example from the same HD shown in panel A of flow cytometry histograms showing the level of NKp46 expression, expressed as mean fluorescence intensity (MFI), after eight days in culture with IL-15 + IL+18 (MFI) on cCD56^{bright} (blue line) and uCD56^{dim} (red line) natural killer (NK) cells derived either from FACS-sorted cCD56^{bright} NK cells (blue) or from FACS-sorted uCD56^{dim} NK cells (red). Overlaid gray histograms represent the level of NKp46 expression on the relative freshly purified and FACS-sorted parental NK cells. (C) Summary statistical graph showing the kinetic of NKp46^{pos}/cCD56^{bright} (blue) and of NKp46$^{neg-low}$/uCD56^{dim} (red) NK cell subsets generated from FACS-sorted cCD56^{bright} (upper graph) and uCD56^{dim} (lower graph) from seven healthy donors. No data are available in panels B and C for cCD56^{dim} NK cells, as they were not proliferating in response to IL-15 and IL-18. Data are expressed as means ± S.D. *P<0.05; ***P<0.001.

we found the degree of CD107a degranulation against K562 cell line of uCD56^{dim} cells purified from hHSCT recipients after six weeks from transplant is significantly lower compared to that of their counterparts from healthy donors (Figure 7A,B).

Considering that the cytolytic activity of NK cells is licensed by the dominant regulation of iNKRs over aNKRs,[10,11] we screened the expression of a large panel of inhibitory receptors, over time, that could likely explain the anergy of donor-derived uCD56^{dim} NK cells from
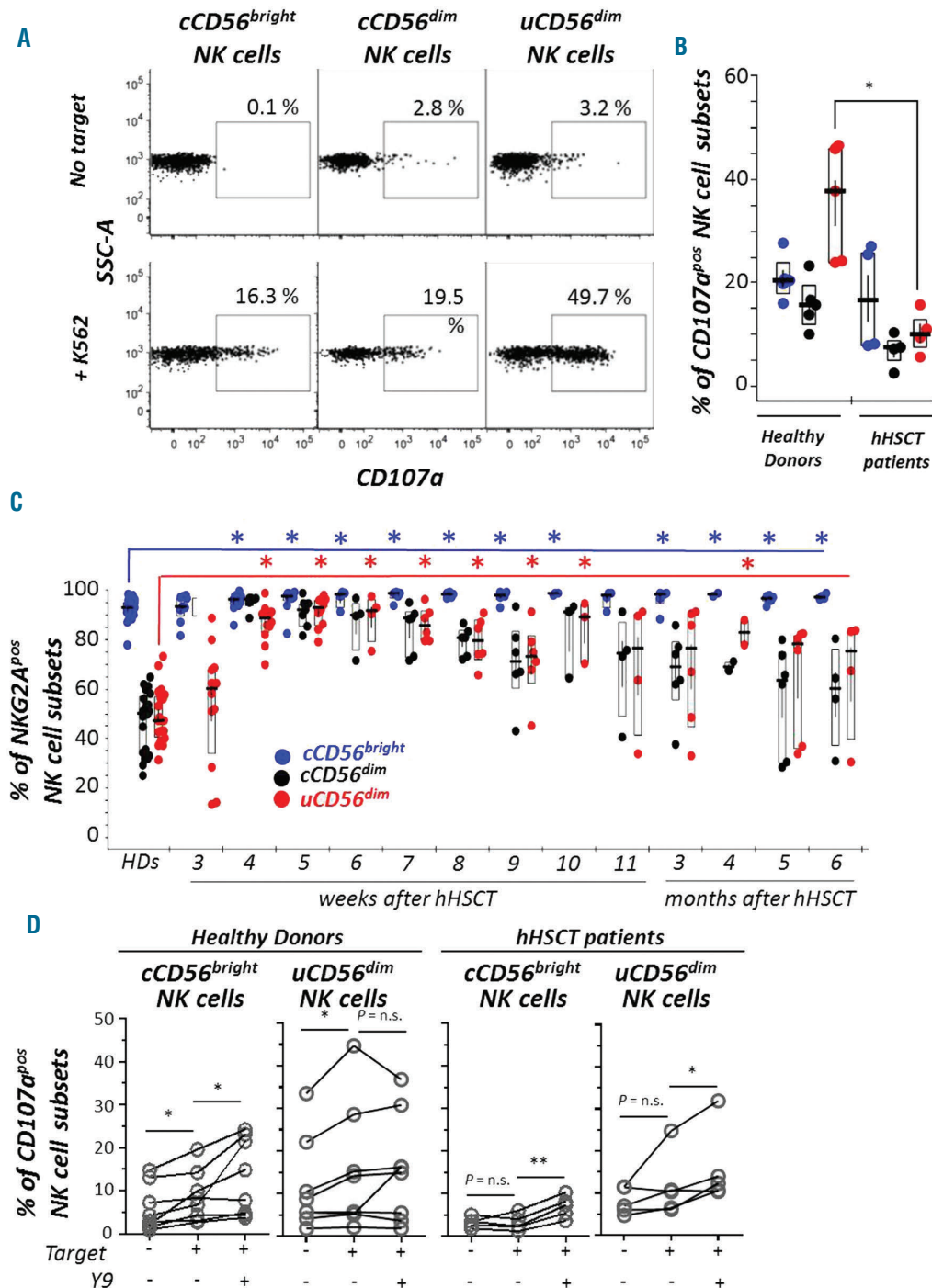

Figure 7. Cytotoxicity of NKp46[neg-low]/uCD56^{dim} from hHSCT patients expressing transient high levels of NK2A early after hHSCT. A) Representative example from a healthy donor (HD) (lower line) of flow cytometry dot plots showing the expression of CD107a (i.e., cytotoxic natural killer [NK] cells) on cCD56^{bright} (left), cCD56^{dim} (middle) and uCD56^{dim} (right) (left column) either in the absence (upper line) or in the presence (lower line) of K562. (B) Summary statistical graph showing the percentage of CD107a^{pos} (median ± SEM) on cCD56^{bright} (blue), cCD56^{dim} (black) and uCD56^{dim} (red) from five HDs and four patients after six weeks from haploidentical HSCT (hHSCT). The background of CD107a^{pos} NK cells present in the spontaneous degranulation has been subtracted for the analyses performed in the presence of K562 cell line. (C) Summary statistical graph showing the expression of NKG2A on cCD56^{bright} (blue), cCD56^{dim} (black) and uCD56^{dim} (red) from HSC HDs and their recipients at different time points up to six months after hHSCT (medians ± SEM). (D) Summary statistical graph showing the percentage of CD107a^{pos} (median ± SEM) on cCD56^{bright} and uCD56^{dim} NK cells from eight HDs and five patients after six weeks from hHSCT alone (-) or incubated (+) with 721.221G cell line, and either in the absence (-) or in the presence (+) of the masking anti-CD94/NKG2A mAb (Y9). *P<0.05; **P<0.01. ns: not significant.

hHSCT recipients. We found that the NK cell expression of CD94/NKG2A is remarkably increased after hHSCT. In particular, while only a fraction (median of 47,2 %±2,5 %) of uCD56^{dim} NK cells from healthy donors is NKG2A^{pos}, almost all uCD56^{dim} NK cells expanded after hHSCT express this iNKR. The significant higher frequency of NKG2A^{pos}/uCD56^{dim} NK cells in the PB of recipients compared to their related healthy donors is detectable between the fourth and eleventh week following hHSCT (Figure 7C).

To understand if this high and transient expression of CD94/NKG2A on donor-derived uCD56^{dim} NK cells reconstituting the recipients could explain their defective cytotoxicity, we performed masking experiments by blocking this iNKR in the presence of a tumor cell line expressing its putative ligand HLA-E (i.e., 721-221G cell line).[35,36] Both cCD56^{bright} and uCD56^{dim} NK cells from healthy donors are able to efficiently degranulate, and the masking with an anti-CD94/NKG2A mAb increased the expression of CD107a only in cCD56^{bright}, in line with their high constitutive expression of NKG2A. In contrast, both cCD56^{bright} and uCD56^{dim} NK cells purified from hHSCT after six weeks from the transplant are not able to efficiently degranulate against 721-221G, and only the blocking of the CD94/NKG2A inhibitory checkpoint significantly increases the expression of CD107a of these NK cell subsets (Figure 7D).

Discussion

The recent development of TCRe-NMAC-PT/Cy hHSCT with RIC represented a revolution in the field of BMT for the cure of hematologic malignancies.[1,2,37] The study herein characterizes the transient and early expansion of a functionally exhausted subset of donor-derived uCD56^{dim} NK cells that is detectable at a high frequency from the second week after the transplant. uCD56^{dim} NK cells are by far the largest NK cell population in the first weeks after hHSCT and are also characterized by a significant higher expression of CD94/NKG2A compared to their counterparts in healthy donors. The increased surface levels of this iNKR early after hHSCT greatly impairs the cytotoxicity of uCD56^{dim} NK cells, thus affecting those
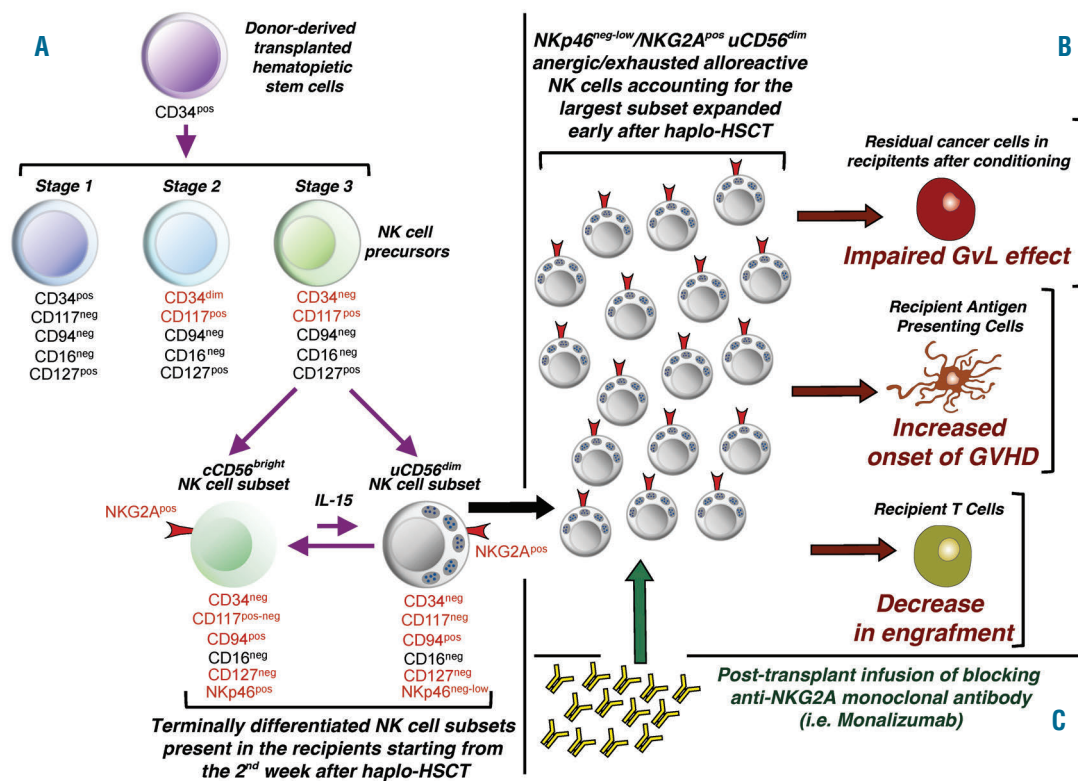

Figure 8. NK cell immune-reconstitution after haploidentical HSCT. (A) Natural killer (NK) cell ontogenesis (left): after the infusion of unmanipulated graft in non myeloablative haplo- hematopoietic stem cells transplant (hHSCT), the reconstitution of NK cells in recipients is completely donor-dependent and starts from CD34^{pos} hematopoietic stem cells. Indeed, mature NK cells infused with the graft do not survive the PT infusion of cyclophosphamide.[25] The first NK cell subsets to be detected starting from the second week after hHSCT are the cCD56^{bright} and uCD56^{dim} NK cells, with the latter population being by far the largest one, expanded early in the first weeks after the transplant. cCD56^{bright} and uCD56^{dim} cells are not NK cell precursors and are able to exert a bi-directional differentiation following stimulation with IL-15, a pro-inflammatory cytokine present at high levels in the sera of lymphopenic recipients in the first weeks after allogeneic transplant.[25,31] (B) Clinical impact (lower right): due to the high constitute expression of the inhibitory receptor NKG2A, uCD56dim NK cells are exhausted in their cytolic potential, and this impairment greatly affects: i) the clearance of residual malignant cells in the recipient that survived the conditioning regimens (i.e., decreased graft-versus-leukemia (GvL) effect), ii) the killing of recipient antigen presenting cells (APCs) presenting host antigens to donor T cells (i.e., increase in the onset of graft-versus-host disease [GvHD]), and iii) the elimination of recipient immune T cells that survived the conditioning regimens (i.e., decrease in engraftment).[7] (C) Therapeutic insights (upper right): the blocking of the NKG2A inhibitory checkpoint unleashes donor-derived NK cell cytotoxicity and increases their alloreactive potential. Hence, the PT infusion of the humanized anti-NKG2A monoclonal antibody (i.e., Monalizumab) represents a potential novel therapeutic approach to improve the clinical outcome of hHSCT.

alloreactive NK cell effector functions that are required for a positive clinical outcome of allogeneic HSCTs (Figure 8).

It has recently been reported the PT/Cy in hHSCT kills all mature and high proliferating NK cells infused in the recipient with the graft. Indeed, NK cells do not express aldehyde dehydrogenase, thus implying that the immature CD62L^{pos}/NKG2A^{pos}/KIR^{neg} NK cells reconstituting in the recipients derive from donor HSCs.[25] Nonetheless, the kinetic and the clinical impact of NK cell subset distribution in this transplant setting are unknown. Even though the absolute numbers of donor-derived NK cells are restored in the recipients few weeks after the transplant, we show herein that the distribution of their subset takes much longer to acquire a pattern similar to that observed in healthy donors.[13] In particular, hHSCT recipients either lack, or have very low frequencies, of circulating cCD56^{dim} NK cells soon after the transplant. The lack of the main cytolytic population that normally accounts for up to 90% of all circulating NK cells is compensated by the expansion, starting from the second week after hHSCT of uCD56^{dim} NK cells, that appear before cCD56^{dim} NK cells and that are present at a higher frequency compared to cCD56^{bright} NK cells early after the transplant.

These findings prompted us to first hypothesize that uCD56^{dim} NK cells might represent an additional stage of NK cell differentiation preceding the appearance of cCD56^{bright} and cCD56^{dim} cell subsets. By focusing our analyses on the different transcriptional profiles of NK cell subsets from healthy donors, we first highlighted the peculiar signature of the uCD56^{dim} NK cell subset. These data made it possible to understand how recipients are repopulated over time by specific subsets of donor-derived NK cells that are affected by the peculiar lymphopenic environment early after hHSCT, and follow a kinetic highly impacting the functional outcome of the transplant. Indeed, both our transcriptional profiles and phenotypic analyses in healthy donors and hHSCT recipients showed that uCD56^{dim} lymphocytes are *bona fide* NK cells and not NK cell precursors, are not an artifact of cryopreservation, and express surface markers of late differentiation such as NKG2D and NKp30 as well as lytic granules indicative of a cytotoxic phenotype. Our results are in line with previous studies showing that uCD56^{dim} NK cells in healthy donors, although present at a very low frequency, represent a distinct subset able to efficiently kill tumor cell targets.[15-17] It has also been reported that the lack or decreased expression of CD16 on activated and degranulating cCD56^{dim} NK cells is mediated by the metalloproteinase-17 (ADAM17), thus potentially explaining, at least in part, the origin of uCD56^{dim} NK cells.[38,39] Considering that mature and highly proliferating NK cells infused with the graft do not survive to the PT/Cy,[25] it is highly unlikely that the action of ADAM17 on activated cCD56^{dim} NK cells could alone explain the high frequencies of uCD56^{dim} NK cells early after hHSCT. Indeed, the expansion of this latter circulating NK cell subset has its peak in the first weeks after hHSCT, when cCD56^{dim} NK cells are either undetectable or present at very low frequencies (Figure 1C,D). Moreover, uCD56^{dim} NK cells are characterized by a remarkably high degree of cellular proliferation in response to cytokine activation, are able to generate cCD56^{bright} NK cells, and express a NKp46[neg-low] phenotype. These functional and phenotypic features do not belong to terminally differentiated cCD56^{dim} NK cells and are neither induced nor mediated by mechanisms associated with ADAM17 cleavage properties. As a matter of fact, we did not find any difference in the transcriptional levels of ADAM17 between cCD56^{dim} and uCD56^{dim} NK cells purified early after hHSCT (*data not shown*). Taken together, these data indicate that ADAM17 likely plays a minor role, if any, in the expansion of uCD56^{dim} NK cells early in hHSCT.

In the context of the cytokine storm characterizing the systemic lymphopenic environment early after allogeneic HSCT (including hHSCT), IL-15 certainly plays a key role as it is highly increased in patients' sera in the first week after the transplant.[25,31] Indeed, the incubation *in vitro* with IL-15 plus IL-18 of FACS-sorted NKp46[neg-low]/uCD56^{dim} purified from healthy donors induces their proliferation and preferential differentiation into NKp46^{pos}/cCD56^{bright} NK cells over time. Only a minor fraction of proliferating uCD56^{dim} NK cells retains its parental phenotype following activation. Additionally we found that, although to a lesser and not statistically significant extent, a small fraction of highly proliferating FACS-sorted NKp46^{pos}/cCD56^{bright} NK cells generate NKp46[neg-low]/uCD56^{dim} NK cells. While these results demonstrate that NKp46 represents an additional surface marker that distinguishes uCD56^{dim} NK cells from both cCD56^{bright} and cCD56^{dim} NK cells, they leave unanswered the question regarding the origin of uCD56^{dim} NK cells. Nonetheless, they indicate the presence of a bi-directional differentiation between this latter subset and cCD56^{bright} NK cells in an *ex vivo* human setting mimicking a lymphopenic environment highly enriched with IL-15. We are certainly aware that this methodological approach does not resemble the complex cellular and molecular interactions occurring in the human BM niche during lymphopoiesis. Indeed, neither uCD56^{dim} nor cCD56^{bright} NK cells were able to generate terminally-differentiated cCD56^{dim} NK cells, a process that requires the presence of additional signals delivered by fibroblasts, mesenchymal and stromal cells.[40-42] However, herein we clearly show that both proliferating uCD56^{dim} and cCD56^{bright} NK cells can generate either themselves or their "neighbor" NK cell subset. In this context, the high serum level of IL-15 soon after hHSCT[25] could also be manipulated to boost a more potent anti-tumor response by cCD56^{bright} NK cells, as recently demonstrated in multiple myeloma.[43] Further studies are needed in order to disclose the mechanisms that finely tune the bi-directional transition between uCD56^{dim} and cCD56^{bright}, both under physiologic conditions and in the lymphopenic setting following allogeneic HSCTs.

Herein, we also demonstrate that the transcriptional profile of uCD56^{dim} NK cells expanded early after hHSCT is distinct from that of their counterparts in healthy donors. This is not surprising in the context of an allogeneic transplant where different stimuli, such as lymphopenia, alloreactivity, a high serum level of cytokines, antigen stimulation, opportunistic viral infections and acute GvHD highly influences the quantity and the quality of IR.[1,24,25] Indeed, this peculiar systemic environment induces the preferential expansion starting from the second week after hHSCT of uCD56^{dim} NK cells which, although showing a cytotoxic phenotype, are highly defective in the clearance of tumor cell targets. This cellular functional exhaustion is associated, at least in part, with the transient expression of CD94/NKG2A on all uCD56^{dim} NK cells that account for the majority of the NK cell population within the first weeks following trans-

plant. Indeed, the blocking of CD94/NKG2A with a masking mAb significantly increased the CD107a degranulation as a marker of lytic activity of NK cells purified early after hHSCT. Although the mechanism(s) inducing the expansion of anergic NKG2A^{pos}/uCD56^{dim} NK cells is unknown, this acquired knowledge now makes it possible to develop a therapeutic approach targeting a specific immune check-point whose inhibition can efficiently increase NK cell alloreactivity within a given time-frame after hHSCT. In this regard, the efficacy of the *in vivo* administration of an anti-CD94/NKG2A blocking mAb (i.e., Monalizumab) in improving NK cell cytotoxicity against solid tumors and leukemic cells has been already reported both in mice and humans.[44,45] (*clinicaltrials.gov Identifier: 02459301*) (Figure 8).

Acknowledgments

Funding

References

1. Patriarca F, Luznik L, Medeot M, et al. Experts' considerations on HLA-haploidentical stem cell transplantation. Eur J Haematology. 2014;93(3):187-197.
2. Luznik L, O'Donnell PV, Symons HJ, et al. HLA-haploidentical bone marrow transplantation for hematologic malignancies using nonmyeloablative conditioning and high-dose, posttransplantation cyclophosphamide. Biol Blood Marrow Transplant. 2008;14(6):641-650.
3. Brunstein CG, Fuchs EJ, Carter SL, et al. Alternative donor transplantation after reduced intensity conditioning: results of parallel phase 2 trials using partially HLA-mismatched related bone marrow or unrelated double umbilical cord blood grafts. Blood. 2011;118(2):282-288.
4. Castagna L, Crocchiolo R, Furst S, et al. Bone marrow compared with peripheral blood stem cells for haploidentical transplantation with a nonmyeloablative conditioning regimen and post-transplantation cyclophosphamide. Biol Blood Marrow Transplant. 2014;20(5):724-729.
5. Imamura M, Tanaka J. Immunoregulatory cells for transplantation tolerance and graft-versus-leukemia effect. Int J Hematol. 2003;78(3):188-194.
6. Ruggeri L, Capanni M, Urbani E, et al. Effectiveness of donor natural killer cell alloreactivity in mismatched hematopoietic transplants. Science. 2002; 295(5562):2097-2100.
7. Moretta L, Locatelli F, Pende D, Marcenaro E, Mingari MC, Moretta A. Killer Ig-like receptor-mediated control of natural killer cell alloreactivity in haploidentical hematopoietic stem cell transplantation. Blood. 2011;117(3):764-771.
8. Vivier E, Raulet DH, Moretta A, et al. Innate or adaptive immunity? The example of natural killer cells. Science. 2011;331(6013):44-49.
9. Ljunggren HG, Karre K. In search of the 'missing self': MHC molecules and NK cell recognition. Immunol Today. 1990; 11(7):237-244.
10. Moretta A, Bottino C, Vitale M, et al. Activating receptors and coreceptors involved in human natural killer cell-mediated cytolysis. Annu Rev Immunol. 2001; 19:197-223.
11. Lanier LL. NK cell recognition. Annu Rev Immunol. 2005;23:225-74.
12. Castagna L, Mavilio D. Re-discovering NK cell allo-reactivity in the therapy of solid tumors. J Immunother Cancer. 2016;4:54.
13. Cooper MA, Fehniger TA, Caligiuri MA. The biology of human natural killer-cell subsets. Trends Immunol. 2001;22(11):633-640.
14. Lugli E, Marcenaro E, Mavilio D. NK cell subset redistribution during the course of viral infections. Front Immunol. 2014;5:390.
15. Takahashi E, Kuranaga N, Satoh K, et al. Induction of CD16+ CD56bright NK cells with antitumour cytotoxicity not only from CD16- CD56bright NK Cells but also from CD16- CD56dim NK cells. Scand J Immunol. 2007;65(2):126-138.
16. Fan YY, Yang BY, Wu CY. Phenotypically and functionally distinct subsets of natural killer cells in human PBMCs. Cell Biol Int. 2008;32(2):188-197.
17. Penack O, Gentilini C, Fischer L, et al. CD56dimCD16neg cells are responsible for natural cytotoxicity against tumor targets. Leukemia. 2005;19(5):835-840.
18. Stabile H, Nisti P, Morrone S, et al. Multifunctional human CD56 low CD16 low natural killer cells are the prominent subset in bone marrow of both healthy pediatric donors and leukemic patients. Haematologica. 2015;100(4):489-498.
19. Helena S, Paolo N, Giovanna P, et al. Reconstitution of multifunctional CD56lowCD16low natural killer cell subset in children given alpha/beta T cell-depleted HLA-haploidentical haematopoietic stem cell transplantation. Oncoimmunology. 2017;9(9):e1342024.
20. Raiola A, Dominietto A, Varaldo R, et al. Unmanipulated haploidentical BMT following non-myeloablative conditioning and post-transplantation CY for advanced Hodgkin's lymphoma. Bone Marrow Transplant. 2014;49(2):190-194.
21. Roberto A, Castagna L, Gandolfi S, et al. B-cell reconstitution recapitulates B-cell lymphopoiesis following haploidentical BM transplantation and post-transplant CY. Bone Marrow Transplant. 2015;50(2):317-319.
22. Roberto A, Castagna L, Zanon V, et al. Role of naive-derived T memory stem cells in T-cell reconstitution following allogeneic transplantation. Blood. 2015;125(18):2855-2864.
23. Gupta N, Arthos J, Khazanie P, et al. Targeted lysis of HIV-infected cells by natural killer cells armed and triggered by a recombinant immunoglobulin fusion protein: implications for immunotherapy. Virology. 2005;332(2):491-497.
24. Imamura M, Tsutsumi Y, Miura Y, Toubai T, Tanaka J. Immune reconstitution and tolerance after allogeneic hematopoietic stem cell transplantation. Hematology. 2003; 8(1):19-26.
25. Russo A, Oliveira G, Berglund S, et al. NK cell recovery after haploidentical HSCT with posttransplant cyclophosphamide: dynamics and clinical implications. Blood. 2018;131(2):247-262.
26. Dulphy N, Haas P, Busson M, et al. An unusual CD56(bright) CD16(low) NK cell subset dominates the early posttransplant period following HLA-matched hematopoietic stem cell transplantation. J Immunol. 2008;181(3):2227-2237.
27. Lugthart G, van Ostaijen-ten Dam MM, van Tol MJ, Lankester AC, Schilham MW. CD56(dim)CD16(-) NK cell phenotype can be induced by cryopreservation. Blood. 2015;125(11):1842-1843.
28. Amir el AD, Davis KL, Tadmor MD, et al. viSNE enables visualization of high dimensional single-cell data and reveals phenotypic heterogeneity of leukemia. Nat Biotechnol. 2013;31(6):545-552.
29. Yu J, Freud AG, Caligiuri MA. Location and cellular stages of natural killer cell development. Trends Immunol. 2013;34(12):573-582.
30. Scoville SD, Freud AG, Caligiuri MA.

Modeling human natural killer cell development in the era of innate lymphoid cells. Front Immunol. 2017;8:360.

31. Melenhorst JJ, Tian X, Xu D, et al. Cytopenia and leukocyte recovery shape cytokine fluctuations after myeloablative allogeneic hematopoietic stem cell transplantation. Haematologica. 2012;97(6):867-873.

32. Mattiola I, Pesant M, Tentorio PF, et al. Priming of human resting NK cells by autologous M1 macrophages via the engagement of IL-1β, IFN-β, and IL-15 pathways. J Immunol. 2015; 195(6):2818-2828.

33. Novick D, Kim S, Kaplanski G, Dinarello CA. Interleukin-18, more than a Th1 cytokine. Semin Immunol. 2013;25(6):439-448.

34. Granzin M, Wagner J, Kohl U, Cerwenka A, Huppert V, Ullrich E. Shaping of natural killer cell antitumor activity by ex vivo cultivation. Front Immunol. 2017;8:458.

35. Lee N, Llano M, Carretero M, et al. HLA-E is a major ligand for the natural killer inhibitory receptor CD94/NKG2A. Proc Natl Acad Sci U A. 1998;95(9):5199-5204.

36. Pesce S, Carlomagno S, Moretta A, Sivori S, Marcenaro E. Uptake of CCR7 by KIR2DS4(+) NK cells is induced upon recognition of certain HLA-C alleles. J Immunol Res. 2015;2015:754373.

37. Blaise D, Furst S, El Cheikh J, et al. Comparison of haploidentical T-replete HSCT followed with post-transplant high dose cyclophosphamide (PT-HDCy) with matched related (MRD) or unrelated (UD) HSCT in patients in or after the 6TH decade. Biol Blood Marrow Transplant. 2015;21(2):S273-S274.

38. Romee R, Foley B, Lenvik T, et al. NK cell CD16 surface expression and function is regulated by a disintegrin and metalloprotease-17 (ADAM17). Blood. 2013; 121(18):3599-3608.

39. Lajoie L, Congy-Jolivet N, Bolzec A, et al. ADAM17-mediated shedding of FcgammaRIIIA on human NK cells: identification of the cleavage site and relationship with activation. J Immunol. 2014; 192(2):741-751.

40. Chan A, Hong DL, Atzberger A, et al. CD56bright human NK cells differentiate into CD56dim cells: role of contact with peripheral fibroblasts. J Immunol. 2007;179(1):89-94.

41. Boissel L, Tuncer HH, Betancur M, Wolfberg A, Klingemann H. Umbilical cord mesenchymal stem cells increase expansion of cord blood natural killer cells. Biol Blood Marrow Transplant. 2008; 14(9):1031-1038.

42. Hosseini E, Ghasemzadeh M, Kamalizad M, Schwarer AP. Ex vivo expansion of CD3depleted cord blood-MNCs in the presence of bone marrow stromal cells; an appropriate strategy to provide functional NK cells applicable for cellular therapy. Stem Cell Res. 2017;19:148-155.

43. Wagner JA, Rosario M, Romee R, et al. CD56bright NK cells exhibit potent antitumor responses following IL-15 priming. J Clin Invest. 2017;127(11):4042-4058.

44. Ruggeri L, Urbani E, Andre P, et al. Effects of anti-NKG2A antibody administration on leukemia and normal hematopoietic cells. Haematologica. 2016;101(5):626-633.

45. McWilliams EM, Mele JM, Cheney C, et al. Therapeutic CD94/NKG2A blockade improves natural killer cell dysfunction in chronic lymphocytic leukemia. Oncoimmunology. 2016;5(10):e1226720.